UDC: 621

ISSN 1451-2092

University of Belgrade
Faculty of Mechanical Engineering

FME TRANSACTIONS

New Series, Volume 44, Number 2, 2016

FME TRANSACTIONS

Published by:
University of Belgrade
Faculty of Mechanical Engineering

On line service:
http:/www.mas.bg.ac.rs/transactions

ISSN 1451-2092 UDC: 621

Volume 44, No 2, 2016, pp. 109 – 216

CONTENTS

PAGE

Milan M. Petrovic, Vladimir D. Stevanovic 109
Two-Component Two-Phase Critical Flow

Mirko S. Kozic, Slavica S. Ristic, Suzana Lj. Linic, Toni Hil, Srdja Stetić-Kozic 115
Numerical Analysis of Rotational Speed Impact on Mixing Process in a Horizontal Twin-Shaft Paddle Batch Mixer with Non-Newtonian Fluid

Ivan Božić, Radiša Jovanović 125
Prediction of Double-Regulated Hydraulic Turbine On-Cam Energy Characteristics by Artificial Neural Networks Approach

M.Kanthababu, Rajes Ram M, Peter Nithin Emannuel, R Gokul, Radhik Rammohan 133
Experimental Investigations on Pocket Milling of Titanium Alloy Using Abrasive Water Jet Machining

T.G. Loganathan, R. Krishna Murthy, K. Chandrasekaran 139
Damage Characterization of GFRP Composite on Exposure to Cyclic Loading by Acoustic Emission

Ana Pavlovic, Francesco Ubertini 146
Equipment Qualification in Testing the Flexural Resistance of Bended Ceramic Tiles

Marko Ristic, Radica Prokic-Cvetkovic, Mirko Kozic, Slavica Ristic, Mirko Pavisic 154
Numerical Simulation of Multiphase Flow Around Suction Plates of Ventilation Mill in the Function of Extending its Remaning Working Life

Srđan Živković 159
NX CAM Post Processing Errors: Machine Data File Generator vs. Post Builder

Milan S. Cajić, Mihailo P. Lazarević 165
Determination of Joint Reactions in a Rigid Multibody System, Two Different Approaches

Michael Eder, Georg Kartnig 174
Throughput Analysis of S/R Shuttle Systems and Ideal Geometry for High Performance

Purnomo, Rudy Soenoko, Agus Suprapto, Yudy Surya Irawan 180
Impact Fracture Toughness Evaluation by Essential Work of Fracture Method in High Density Polyethylene Filled with Zeolite

M. P. Nagarkar, G. J. Vikhe Patil 187
Multi-Objective Optimization of LQR Control Quarter Car Suspension System using Genetic Algorithm

Rajesh M. Darji, Munir G. Timol 197
Similarity treatment for MHD free convective boundary layer flow of a class of Non-Newtonian Fluids

Radoslav Z. Rajković, Nenad Đ. Zrnić, Snežana D. Kirin, Branislav M. Dragović 204
A Review of Multi-Objective Optimization of Container Flow Using Sea and Land Legs Together

Milena Papić-Obradović, Branislava Jeftić, Lidija Matija 212
Papanicolaou Stained Cervical Smear Analysis Using Opto-Magnetic Imaging Spectroscopy

l_{rack}	length of the rack
v_{lift}	velocity of the lift
$v_{shuttle}$	velocity of the shuttle
a_{lift}	acceleration of the lift
$a_{shuttle}$	acceleration of the shuttle
$t_{load/unload\_lift}$	loading/unloading time of the lifts
$t_{load/unload\_shuttle}$	loading/unloading time of the shuttles
$w_{restore}$	probability for restoring a container
$t_{restore}$	expected time for restoring a container
n	number of storage levels
K	capacity of the queuing system

Greek symbols

ϑ	throughput of a storage level
ϑ_{system}	throughput of the whole shuttle system
ρ	utilization rate
λ	arrival rate
μ	service rate

АНАЛИЗА КАПАЦИТЕТА СКЛАДИШНИХ ШАТЛ СИСТЕМА И ИДЕАЛНА ГЕОМЕТРИЈА ЗА ДОСТИЗАЊЕ ВИСОКИХ ПЕРФОРМАНСИ

М. Едер, Г. Картниг

Шатл системи се примењују код аутоматизованих складишних система високих перформанси за јединичне терете. Сваки ниво складишта се опслужује једним транспортним возилом. Постоји лифт за складиштење на предњој страни складишног система. Између лифтова и одговарајућих нивоа постоји различит број међупростора. Овакви системи су већ били коришћени у различитим научним радовима, а постоје и VDI препоруке, али само за аналитички приступ са задовољавајућом тачношћу. Проблем који се јавља код свих метода за описивање шатл система је геометрија регала. Код аутоматизованих складишних система за јединичне терете основна геометрија ходника складишта је критична са аспекта капацитета. Изложена студија треба да допринесе решавању поменутог проблема.

виши него у условима пражњења. За елемент пражњења овакво стање представља критично оптерећење. Предмет овог рада је одређивање оптерећења и погонске снаге тракастог транспортера на пробном столу. Извршено је поређење резултата прихваћених аналитичких модела, симулације и мерења. Посебно се анализира утицај висине испусног отвора на погонску снагу.

Klaus Decker
Senior Scientist
Vienna University of Technology
Faculty of Mechanical and Industrial Engineering
Austria

Martin Egger
Professor
University of Applied Sciences Upper Austria
School of Engineering and Environmental Sciences
Austria

Alexander Haber
Research Assistant
Vienna University of Technology
Faculty of Mechanical and Industrial Engineering
Austria

Christoph Pillichshammer
R&D Engineer
InoCon Industrial Plants GmbH
Austria

Drive Power of a Discharge Belt Conveyor – Comparison of Calculation, Simulation and Measurement

Usually there is a discharger under the hopper at the bottom of a silo (e.g. discharge belt, discharge screw). It must be able to bear the load of the bulk material and should achieve the intended interaction with the hopper for optimum draw-down.
Immediately after filling the empty hopper, the vertical pressure in the outlet opening is usually higher than in the emptying state. For a discharger this situation represents the critical load.
Subject of this paper is the determination of loads and drive powers of a belt discharger test stand. The results of recognized analytical models, simulation results and measurement results are compared. In particular, the influence of the outlet height on the drive power will be analysed.

Keywords: *discharge belt conveyor, drive power calculation, filling state, DEM simulation, measurement.*

1. INTRODUCTION

Immediately after the filling of an empty silo or bin (filling state) the vertical stress at the outlet is greater than in the case of discharging (discharging state) [1]. Figure 1 illustrates what happens during the filling and discharging of a silo. During filling the height h_f and the vertical stress σ_v at the outlet increase with time. As soon as bulk material is discharged the vertical stress σ_v at the outlet decreases suddenly. That means, that the maximum discharge force F_h occurs in the filling state.

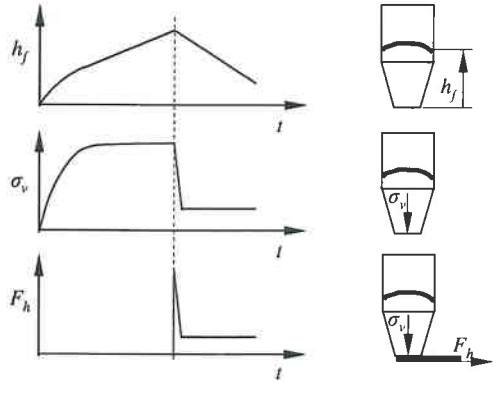

Figure 1. Filling height, vertical stress at the outlet and discharge force vs. time [1]

For the determination of the discharge force there are several analytical models available. The force is dependent on the internal friction of the bulk material, the friction between wall and bulk material as well as the friction resistance of the belt. Forces of inertia are usually neglected because of the low discharge speed.

Received: September 2015, Accepted: May 2016
Correspondence to: Dr. Klaus Decker
Senior Scientist, Vienna University of Technology,
Faculty of Mechanical and Industrial Engineering
E-mail: klaus.decker@tuwien.ac.at
doi:10.5937/fmet1603272D

The aim of this paper is to discover how the outlet height influences the drive power. For this recognized analytical models, DEM simulation results and measurement results are compared. The tests were carried out at a test facility (see figure 2), that was provided by the company INOCON Industrial Plants. The project was funded by the Austrian Research Promotion Agency (FFG).

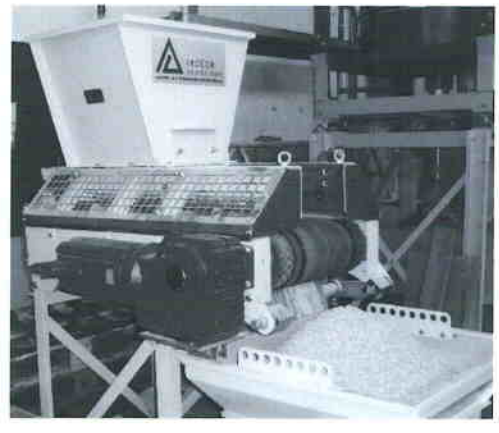

Figure 2. Test facility with a belt conveyor

2. ANALYTICAL EVALUATION

2.1 Vertical stresses

The determination of the discharge forces and drive powers requires the calculation of the vertical stresses in the bin. Three different cases must be taken into consideration:

- Calculation of the stress in the hopper for filling state
- Calculation of the stress in the hopper for discharging state
- Calculation of the stress in the vertical section of the bin

In this paper the slice element method by Janssen [2] was used for the calculation of the stress in the vertical section. The stress in the hopper for filling state was determined with the Motzkus [3] method and for the discharging state the method of Arnold and McLean [4] was used. These methods are applied in the Silo Stress Tool (SSTOOL) of Schulze [5], which is an easy to use software tool for the calculation of stresses in silos and bins, consisting of a vertical section, a hopper below this section, and another vertical section below the hopper.

The slice element method considers a slice-shaped volume element of infinitesimal height dz.

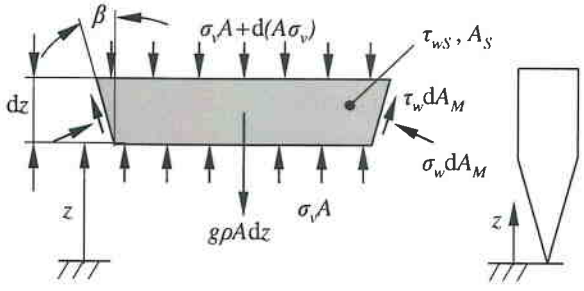

Figure 3. Slice element in the hopper

The equilibrium of forces in z-direction for a wedge-shaped hopper with a small length to width ratio, and therefore with consideration of the friction at the end walls (last term in (1)) yields:

$$\mathrm{d}\{A\sigma_v\} + g\rho A\mathrm{d}z = \sin\beta\sigma_w \mathrm{d}A_M + \\ +\cos\beta\tau_w \mathrm{d}A_M + 2\tau_{wS}\mathrm{d}A_S \tag{1}$$

The ratio of the normal pressure against the wall to the average vertical pressure is expressed by

$$K_h = \sigma_w / \sigma_v \tag{2}$$

The value of K_h is dependent on the mode of operation (filling, discharging). Thus the problem in the application of the equation presented above is the calculation of K_h.

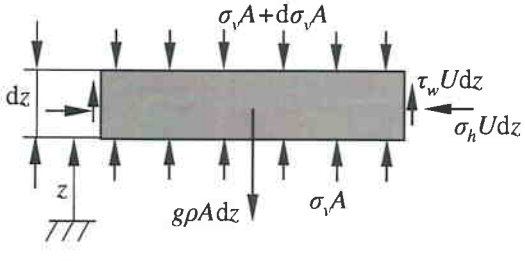

Figure 4. Slice element in the vertical section

For a slice element of the vertical section of the silo the equilibrium of forces in z-direction yields:

$$\mathrm{d}\sigma_v A + g\rho A\mathrm{d}z = \tau_w U\mathrm{d}z \tag{3}$$

The solutions of the differential equations (1) and (3) are not presented in this paper. They can be found in [1-4], [6].

The results of the Silo Stress Tool for the bulk material used are shown in figure 5 and the material data are listed in table 1.

Table 1. Material data of the bulk material

Bulk material: Crushed rock (grain size 4/8 mm)	
Bulk density (ρ)	1320 kg/m³
Effective angle of internal friction (δ)	45°
Angle of wall friction between steel and bulk material (φ_x)	23.5°
Stress ratio ($K_v=\sigma_h/\sigma_v=1.2\cdot[1-\sin(\delta)]$)	0.35

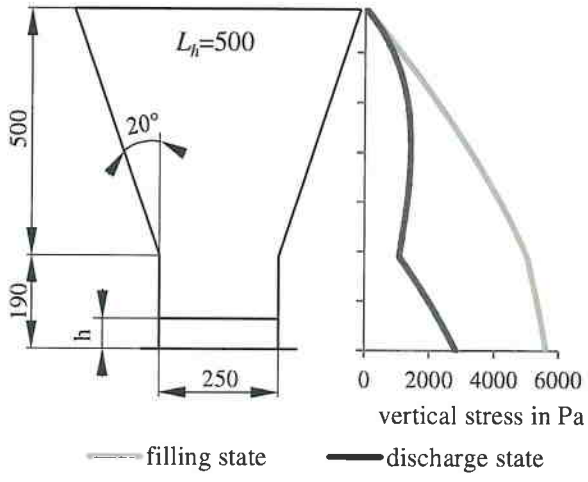

Figure 5. Vertical stress for filling and discharge state

2.2 Forces

The maximum discharge force of the belt conveyor is given by the transmittable frictional force between belt and bulk material

$$F_{h,\max} = \sigma_{vb} L_h b \mu_B \tag{4}$$

where σ_{vb} = vertical stress acting on the belt, L_h = length of the hopper, b = width of the hopper and μ_B = coefficient of wall friction between belt and bulk material.

The force to shear the bulk material is given by [6]

$$F_s = \sigma_{vs} L_h b \mu_E \tag{5}$$

where σ_{vs} = vertical stress in the shear zone and μ_E = equivalent friction coefficient.

Various authors suggest different values for the equivalent friction coefficient μ_E. An expression with respect to the geometry of the shear zone is [7]

$$\mu_E = \frac{\mu_S \cos(\psi) - \sin(\psi)}{\cos(\psi) + \mu_S \sin(\psi)} \tag{6}$$

where ψ is the release angle (see figure 6) and assuming that the maximum shear stress corresponds to the failure condition then the coefficient μ_S of internal friction on the shear plane is normally taken to be [7]

$$\mu_S = \sin(\delta) \tag{7}$$

The skirt plate resistance may be determined as follows:

Hopper section:

$$F_{sph} = K_v \mu_x \left(\frac{\sigma_{vs} + \sigma_{vb}}{2} \right) L_h h \tag{8}$$

where K_v = ratio of lateral to vertical stress at skirt plates, μ_x = coefficient of wall friction and h = height of the outlet.

Guide plate section:

$$F_{spe} = 2K_v\mu_x \frac{\rho g}{2} L_e h^2 \quad (9)$$

where L_e = length of guide plates.

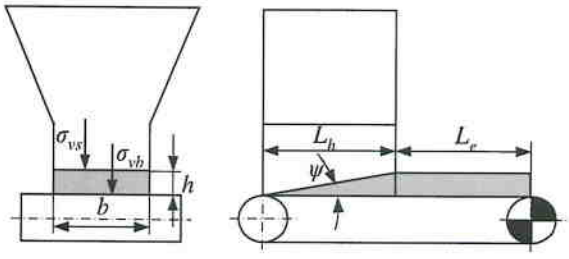

Figure 6. Release angle and other dimesions [6]

The total discharge force is therefore

$$F_h = F_s + F_{sph} + F_{spe} \quad (10)$$

if the condition below for non-slip is fulfilled:

$$F_{h,\max} \geq F_h \quad (11)$$

2.3 Drive power

The drive power is given by

$$P = (F_h + F_{NL})v \quad (11)$$

where F_{NL} = no-load drive force and v = velocity of the belt

2.4 Calculation results

The results of the analytical evaluation of the discharge force and the drive power of the belt conveyor for filling and discharge state are listed in the figure below.

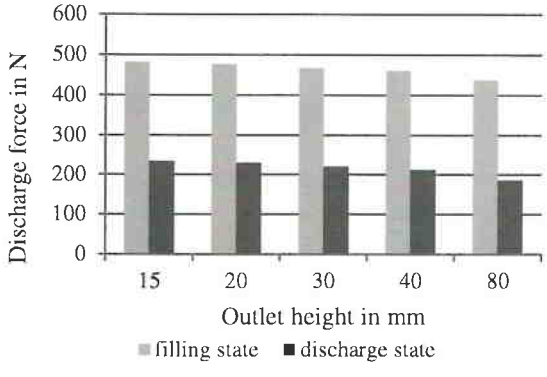

Figure 7. Results of analytical evaluation

3. DISCRETE ELEMENT METHOD SIMULATION

The discrete element method (DEM) is a numerical method for computing the motion of a large number of particles. In a DEM simulation for all particles, a starting position and an initial velocity are specified. The initial data and the appropriate contact model, which describes the behaviour of the particle interaction, make it possible to calculate the forces acting on each particle. All these forces are aggregated. An integration method is employed to compute the change in the position and the velocity of each particle during a certain time step in accordance with Newton's laws of motion. Once the new positions and velocities of each particle have been obtained the forces are recalculated. This loop is repeated until the simulation period is completed.

The default model in EDEM is the Hertz-Mindlin contact model [8], which is also used in this simulation of the discharge belt conveyor. All DEM simulations were performed using the EDEM 2.7 particle simulation software from DEM Solutions Ltd., Edinburgh, Scotland.

3.1 Calibration of the simulation model

The unknown parameters of the Hertz-Mindlin contact models, e.g. rolling friction coefficient, static friction coefficient, coefficient of restitution, were determined by statistical experimental design. For this a Box Behnken experimental design was chosen.

The advantage over other experimental designs, e.g. a full factorial experimental design, is that less testing and evaluation is involved. Five factors (unknown parameters) with three levels of parameter values of a full factorial design requires 243 attempts and the Box Behnken experimental design only 46.

In order to compare the results of experimental designs with measurement results, a test stand was developed [9]. It enables reproducible experiments to be performed simply and easily to describe the bulk behaviour (see shear-slip-fall test in figure 8 and figure 9). For this the shear force F_s, the position of the contact point h_c, the angle of repose β_r and the throughput time can be measured.

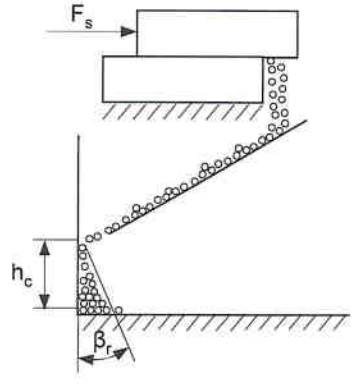

Figure 8. Basic layout of the shear-slip-fall test stand

The individual tests (combinations of parameter values) were simulated by the DEM software EDEM. The analysis of the results of the Box Behnken experimental design was carried out with the help of the statistical software package JMP. The statistical software obtained values for the parameters with the smallest deviations between simulation and measurement.

The tested bulk material (crushed rock) has a grain size of between 4 and 8 mm. To get an idea of the influence of the particle size in the simulation on the

drive power according to the outlet height of the hopper the particle diameter for particle model A was set at 14 mm and for particle model B at 8 mm. In order to obtain timely results all particles in the simulation are spheres of the same size. All values of the simulation parameters are listed in the following table.

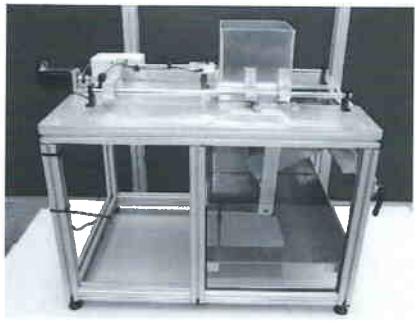

Figure 9. Picture of the shear-slip-fall test stand

3.2 Simulation parameters

Table 2. Values of simulation parameters

		Particle model A	Particle model B
Particle Properties	Diameter	14mm	8mm
	Poisson's Ratio	0.3	0.3
	Shear Modulus	$5*10^9$	$5*10^7$
	Density	2600	2400
Interaction Particle / Particle	Restitution	0.287	0.278
	Static Friction	0.512	0.55
	Rolling Friction	0.1	0.1
Interaction Particle / Steel	Restitution	0.261	0.261
	Static Friction	0.859	0.43
	Rolling Friction	0.36	0.63
Interaction Particle / Belt	Restitution	0.261	0.2
	Static Friction	0.859	0.63
	Rolling Friction	0.36	0.63

3.3 Simulation model

The generated simulation model of the discharge belt conveyor is shown in figure 10. For this purpose, all previously determined properties are used. The motion of the belt is implemented in EDEM as a so-called moving plane. After the bin is filled, the belt accelerates at 0.2s to the specified velocity of 0.2m/s.

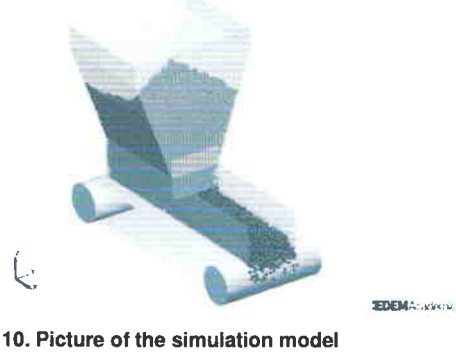

Figure 10. Picture of the simulation model

With a time step of 20% of the Rayleigh time step, the computing time for 10s of simulated real time takes about 10 hours for particle model A and about 37 hours for particle model B.

3.4 Simulation results

In the following the results of the simulation are summarized. Figure 11 shows a section through the discharge belt during the conveying process. The dark particles move in the x-direction at a speed of more than 50% of belt speed. The shear angle previously introduced in the analytical calculation is very easy to recognize.

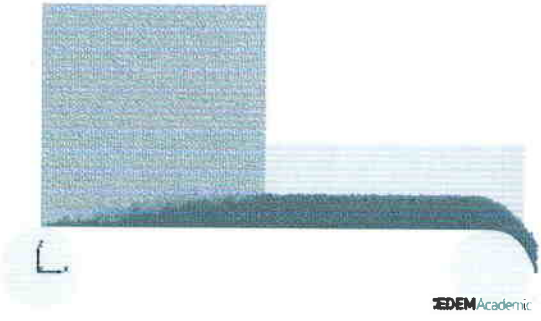

Figure 11. Simulated shear zone

The results for vertical stress and discharge force are shown in Figure 12. In addition to the simulation results, the values determined analytically for the filling and discharge pressure are also entered here.

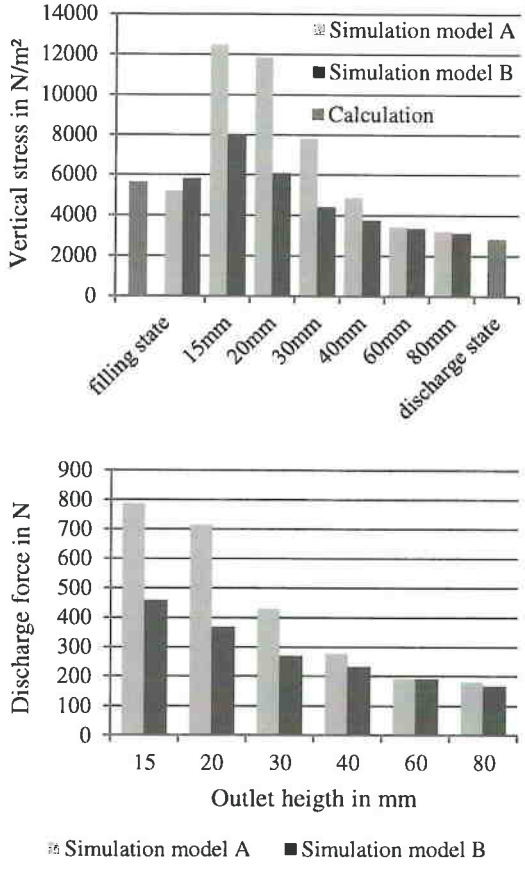

Figure 12. Results of the simulation

In contrast to the measurement results, a large decrease in vertical stress and thus the belt force is now

visible as the gate opening increases. It is also very easy to see the influence of the particle diameter in comparison to the slide opening. While both particle models produce similar results for large openings, the deviation is greater the smaller the outlet height.

In addition, for small slide openings the maximum pressure in the silo occurs in the discharge state but not in the filling state. This is also evident in the two representations in Figure 13. The velocity vectors of those particles whose z-component points upwards are shown in black.

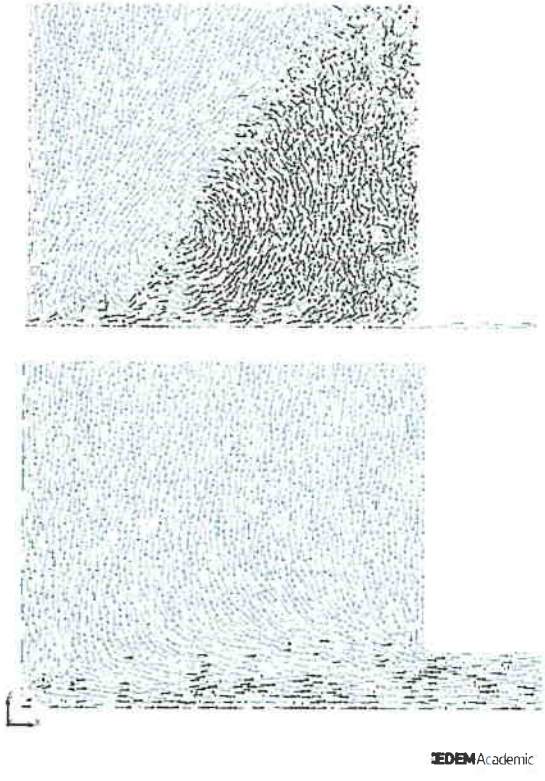

Figure 13. Particle flow inside the bin – 15mm vs. 80mm outlet height

With a large slide opening the bulk material caught at the rear of the conveyor belt can be conveyed through the gate, resulting in a homogeneous particle stream. Otherwise, the bulk material has to be conveyed upwards before the gate, and accumulates there. This causes friction on the walls no longer reducing the pressure downwards but preventing the particles moving to the top, whereby the pressure on the belt is increased.

4. MEASUREMENT RESULTS

The actuation of the belt conveyor of the test facility is effected by a synchronous servo brake motor with electronic frequency converter from SEW, which makes it possible to determine the values for power, torque and velocity. Special software is required to record the measured data. The results of the tests are transferred to the MS Excel spreadsheet program for further processing. Figure 14 shows the measured data for a outlet height of 30mm. In addition to the required total dicharge force, the no-load drive force is also displayed. This is approximately 650N and up to 1700N for the starting process due to the measurement of the active current.

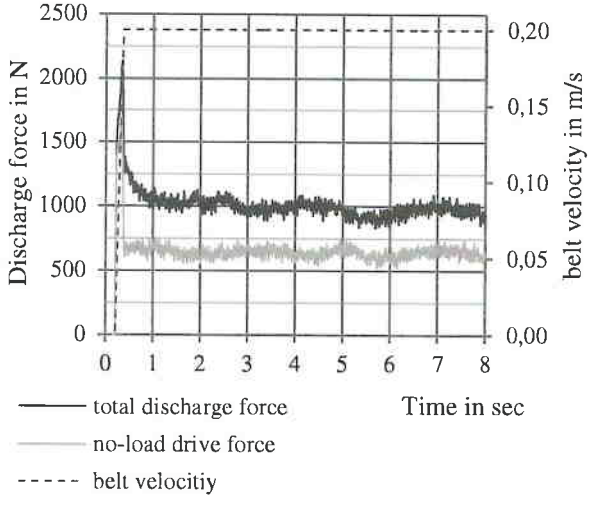

Figure 14. Measurement results for the outlet height of 30mm

5. COMPARISON OF RESULTS

In figure 15 the simulated and the measured driving force are compared over time. For the simulation result the measured no-load drive force is added. Both the starting process and the steady state can be reproduced very well.

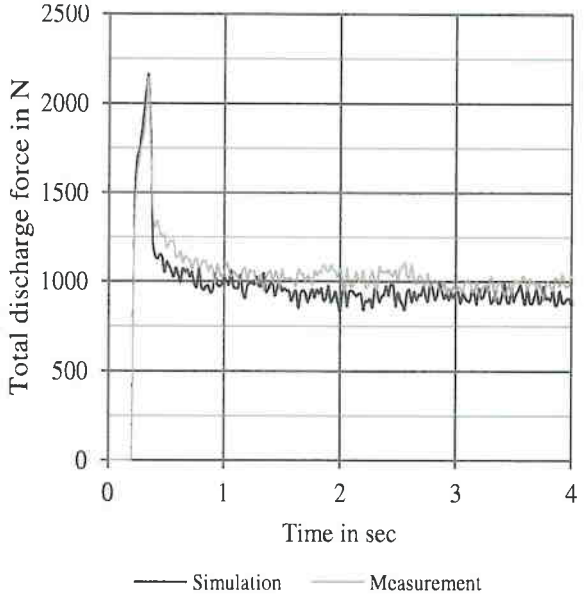

Figure 15. Measurement against simulation over time for the outlet height of 30mm

Finally, Figure 16 shows a comparison of the calculated, simulated and measured results for various slide openings. For the small slide openings, particle model A is too coarse and only produces adequate results for slide openings greater than 40mm. The situation is similar with the analytical calculation. The driving power required for small slide openings can only be determined with sufficient accuracy with the DEM simulation of particle model B.

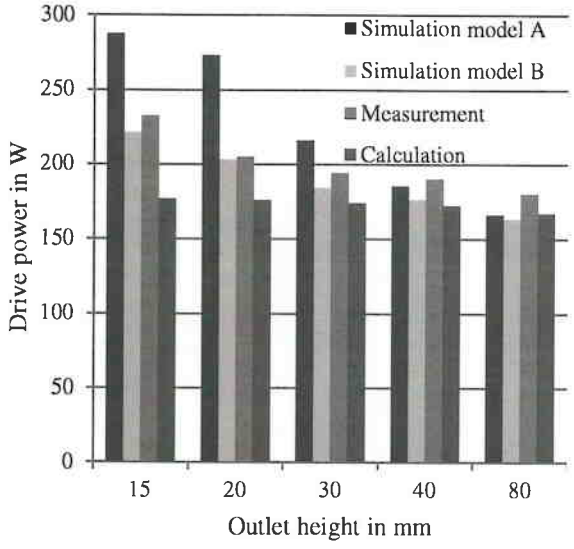

Figure 16. Comparison of results

6. CONCLUSION

It was shown that good concordance is achieved between simulation and measurement, however, the existing computational methods mainly produce results with impermissibly large deviations at small slide openings. It was also found that in the discharge state small slide openings can cause pressures on the belt, which are greater than the filling pressures.

This effect should be investigated in future work and should be prepared for analytical mathematical models. Furthermore, the influence of the hopper outlet geometry would seem to be interesting for further investigations.

REFERENCES

[1] Schulze, D.: *Powders and bulk solids: behavior, characterization, storage and flow*, Springer, Berlin, 2007.

[2] Janssen, H. A.: Getreidedruck in Silozellen, Z. Ver. Dt. Ing., Vol. 39, pp. 1045-1049, 1895.

[3] Motzkus, U.: *Belastung von Siloböden und Auslauftrichtern durch körnige Schüttgüter*, Dissertation TU Braunschweig, 1974.

[4] Arnold, P.C., McLean, A.G.: An analytical solution for the stress function at the wall of a converging channel, Powder Technology, Vol. 13, pp. 279-281, 1976.

[5] Schulze, D.: SILO STRESS TOOL Version 1.2.0.2, http://www.dietmar-schulze.de/downl1c.html, 2014.

[6] Schulze, D.: *Untersuchungen zur gegenseitigen Beeinflussung von Silo und Austragorgan*, Dissertation TU Braunschweig, 1991.

[7] Roberts, A. W.: Recent developments in feeder design and performance, Handbook of Powder Technology, Vol. 10, pp. 211-223, 2001.

[8] *EDEM 2.7 User Guide*, DEM Solutions Ltd., Edinburgh, 2015.

[9] Kalkan, Y.: *Development of a test facility for calibration of DEM models of bulk materials*, Technische Universität Wien, 2013.

NOMENCLATURE

b	width of the hopper
F_h	discharge force
F_{NL}	no-load drive force
F_s	shear force
F_{sph}	skirt plane resistance force under the hopper
F_{spe}	skirt plane resistance force beyond the hopper
h	height of outlet
K_v	ratio of lateral to vertical stress at skirt plates
L_e	length of guide plates
L_h	length of the hopper
v	velocity of the belt

Greek symbols

β	half hopper angle
δ	effective angle of internal friction
μ_B	coefficient of wall friction between belt and bulk material
μ_E	equivalent friction coefficient
μ_S	coefficient of internal friction on shear plane
μ_x	coefficient of wall friction
ρ	bulk density
σ_{vb}	vertical stress acting on the belt
σ_{vs}	vertical stress in the shear zone
ψ	shear zone release angle

ПОГОНСКА СНАГА ТРАКАСТОГ ТРАНСПОРТЕРА ЗА ПРАЖЊЕЊЕ – ПОРЕЂЕЊЕ ИЗРАЧУНАВАЊА, СИМУЛАЦИЈЕ И МЕРЕЊА

К. Декер, М. Егер, А. Хабер, К. Пилихшамер

На дну силоса, испод левка, обично се налази елемент за пражњење (нпр. тракасти транспортер, пужни транспортер). Он мора да има капацитет да носи оптерећење расутог материјала и треба да оствари планирану интеракцију са левком у циљу оптимизације исисавања материјала.

Непосредно после пуњења празног левка, вертикални притисак у испусном отвору је обично